SAND2020-12120J

Biodiesel Ethers: Fatty Acid Derived Alkyl Ether Fuels as Improved

**Bioblendstocks for Mixing-Controlled Compression Ignition Engines** 

Joseph S Carlson<sup>a†</sup>, Eric A Monroe<sup>a†</sup>, Rakia Dhaoui<sup>a</sup>, Junqing Zhu<sup>b</sup>, Charles S McEnally<sup>b</sup>,

Somnath Shinde<sup>a</sup>, Lisa D Pfefferle<sup>b</sup>, Anthe George<sup>a</sup>, Ryan W Davis<sup>a</sup>\*

<sup>a</sup>Department of Biomass Science & Conversion Technologies, Sandia National Laboratories, 7011

East Ave, Livermore, CA 94550

<sup>b</sup>Department of Chemical and Environmental Engineering, Yale University, 9 Hillhouse Avenue,

New Haven, CT 06520

<sup>†</sup>These authors contributed equally.

\*Corresponding author:

E-mail: rwdavis@sandia.gov (Ryan W. Davis)

#### **ABSTRACT**

In the last 20 years, biodiesel consumption in the United States has rapidly increased to ~2B gallons per year as a renewable supplement to fossil fuel. However, further expansion of biodiesel use is currently limited in part by poor cold weather performance which prevents year-round blending and necessitates blend walls ≤5% v/v. In order to provide a diesel fuel blendstock with improved cold weather performance (cloud point, pour point, cold filter plug point), while at the same time maintaining other required fuel performance specifications, several biodiesel analogues were synthesized and tested. These fuels showed improvement in cetane number, lower heating value (LHV), relative sooting tendency, and cold flow properties when compared to a B100 biodiesel composed of the identical fatty acid profile. It was observed as a general trend that the reduced form of biodiesel, fatty alkyl ethers (FAEs), show performance improvements in all fuel property metrics. The suite of improved properties provided by FAEs gives biodiesel producers the opportunity to diversify their portfolio of products derived from lipid and alcohol feedstocks to include long-chain alkyl ethers, a biodiesel alternative with particular applicability for winter weather conditions across the US.

**Keywords**: Biodiesel; ethers; cetane number; cloud point (CP); low-temperature properties; yield sooting index (YSI)

### INTRODUCTION

To support the growing desire to reduce greenhouse gas emissions and establish energy independence, the United States is mandated by federal law to produce 1 billion gallons a year of renewable transportation fuel.¹ While ethanol has emerged as the dominant biofuel for sparkignition engines, biodiesel has become the dominant biofuel for compression ignition engines. Biodiesel is defined as "a fuel comprised of monoalkyl esters of long-chain fatty acids derived from vegetable oils or animal fats, designated B100".² Biodiesel is typically produced by conversion of triglycerides into fatty acid methyl esters (FAMEs) using methanol, where the fatty acid profile of the lipid source will determine the fuel properties. While biodiesel has successfully penetrated the fuel market, with production reaching 2.2 billion gallons in 2016,³ poor performance in important fuel properties such as cold flow continues to limit the application of blend volumes to ≤5% (v/v) in cold weather environments. <sup>4-6</sup> These blend volume restrictions must be overcome in order to maximize the potential for bioderived transportation fuels for diesel engines.

To address these challenges, significant research efforts have been made to discover new bioderived fuels for diesel engines that have improved fuel properties as compared to FAMEs.<sup>7-12</sup> Alkyl ethers have emerged as promising candidates, with recent efforts by Huq et al demonstrating that ethers such as 4-butoxyheptane meet all the basic requirements for a diesel fuel, and can significantly reduce overall CO<sub>2</sub> emissions.<sup>13</sup>

While the fuel properties of alkyl ether compounds are generally established as quite promising for diesel engines, <sup>14, 15</sup> the greatest limitation to industrial scale up may be their preparation. <sup>16</sup> The most well-established methods for making ethers have been catalytic dehydration or Williamson ether synthesis. Both methods have limitations on making asymmetric or hindered ethers, but

recent developments on catalytic Mitsunobu<sup>17</sup> and electrochemical<sup>18</sup> methodologies (coupled with potential renewable electricity availability) are making ether synthesis more routine, increasing the potential for synthetic approaches to biomass derived ether biofuel targets.

In this work, we investigate Fatty Alkyl Ethers (FAEs) as a new biofuel target, which utilizes the same domestic vegetable oil supply as biodiesel, but has a more reduced oxidation state that may improve critical fuel properties such as cold flow, cetane number, heating value, and soot tendency. Additionally, this study investigates the impact of the length and branching of the non-lipid alkyl chain on critical fuel properties in order to maximize the blending ratios of these molecules into petroleum diesel, thereby further reducing carbon emissions from the transportation sector.

### **EXPERIMENTAL SECTION**

#### **Materials**

All molecules investigated in this study were synthesized using a commercial soy FAME sample as the lipid source. The FAME sample was derived from soybean oil, batch #20368, generously provided by Lisa Fouts and Robert McCormick at the National Renewable Energy Laboratory (NREL), with properties and composition detailed by Fioroni et al 2019. The fatty acid profile is shown in **Table 1**. All fuels in this study are a mixture with a fatty acid chain composition identical to that shown in **Table 1**.

**Table 1**. Components of B100 lipid profile used in this study.

Fatty Acids	Myristic	Palmitic	Palmitoleic	Stearic	Oleic	Linoleic	Linolenic	Arachidic	Other
C <sub>total</sub> : C=C	14:00	16:00	16:01	18:00	18:01	18:02	18:03	20:00	
Composition (% w/w) <sup>a</sup>	0.07	10.84	0.27	4.52	23.21	52.73	7.34	0.41	0.61

<sup>&</sup>lt;sup>a</sup>Normalized mass fractions are values based on GCMS analysis of the B100 blend.

This FAME sample is also used as a reference fuel for comparison of fuel properties. Unless otherwise noted, all reactions were carried out in oven-dried glassware sealed with rubber septa under an argon atmosphere with Teflon-coated magnetic stir bars. All reagents were purchased from Sigma Aldrich or Alfa Aesar and were used without further purification unless otherwise stated. All reactions were monitored by TLC, GCMS or NMR analysis. Visualization of analytical thin-layer chromatography was accomplished with UV (254) and potassium permanganate (KMnO<sub>4</sub>) as a staining solution.

## Preparation of FA alcohol

A 2 L round bottom flask was charged with LAH (28.2 g, 0.742 mol, 1.1 equiv.) and Et<sub>2</sub>O (1,350 mL), then cooled to 0 °C with an ice bath. To this mixture, with rapid stirring, **B100** (200.0 g, 0.675 mol, 1.0 equiv.) was added dropwise via addition funnel. The cooling bath was removed, and the mixture was stirred for 2 h. Once starting material was consumed as determined by TLC and GCMS, the reaction was cooled to 0°C and diluted with EtOAc (50 mL) and quenched via slow, sequential addition of H<sub>2</sub>O (28 mL), 10% NaOH (28 mL), and H<sub>2</sub>O (84 mL) which stirred at room temperature for 1 h. To this mixture, anhydrous MgSO<sub>4</sub> was added and stirred for an additional 1 h. The mixture was filtered, and the resulting yellow oil was purified by bulb to bulb distillation (181-189 °C, 1.30 Torr) to provide **FA alcohol** as a colorless oil (163 g, 91%).

## Preparation of FA ethyl ester

A 1 L round bottom flask was charged with **B100** (80.0 grams, 0.270 mol), anhydrous ethanol (160 mL, 2.70 mol) and concentrated H<sub>2</sub>SO<sub>4</sub> (2 mL). The mixture was refluxed for 12 hours. The mixture was cooled and H<sub>2</sub>O was added (100 mL) followed by hexanes (100 mL). The biphasic mixture was separated and the organic layer was washed with saturated aqueous NaHCO<sub>3</sub> (50 mL) then brine (50 mL). The mixture was dried with MgSO<sub>4</sub> and concentrated *in vacuo* to provide **FA ethyl ester** as a clear slightly yellow oil (67.0 grams, 80% yield). <sup>1</sup>H NMR (500 MHz, CDCl<sub>3</sub>)  $\delta$  5.45 – 5.25 (m, 3.1H), 4.12 (q, J = 7.1 Hz, 2H), 2.77 (t, J = 6.7 Hz, 1.4H), 2.28 (t, J = 7.6 Hz, 2H), 2.07 – 1.99 (m, 4H), 1.63 (m, 3H), 1.43 – 1.16 (m, 22H), 0.88 (td, J = 6.7, 4.6 Hz, 3H).

# **Preparation of FA Acetate**

A 500 mL round bottom flask was charged with **FA alcohol** (60.0 grams, 0.225 mol), pyridine (21.8 mL, 1.2 equiv) and DCM (250 mL). The mixture was cooled with an ice bath followed by the addition of acetyl chloride (19.3 mL, 1.2 equiv). The mixture was allowed to warm to room temperature and stirred for 4 hours. H<sub>2</sub>O (250 mL) was added, the biphasic mixture was separated and the aqueous phase was washed with hexanes (3 x 50 mL). The combined organics were washed with water (40 mL) and brine (40 mL) then dried with MgSO<sub>4</sub> and concentrated *in vacuo* to provide **B100 acetate** (41.0 grams, 59% yield) as yellow oil. <sup>1</sup>H NMR (500 MHz, CDCl<sub>3</sub>)  $\delta$  5.44 – 5.27 (m, 2.8H), 4.05 (t, J = 6.8 Hz, 2H), 2.77 (t, J = 6.7 Hz, 1.3H), 2.04 (m, 6H), 1.61 (t, J = 7.1 Hz, 2H), 1.42 – 1.19 (m, 19H), 0.88 (td, J = 6.9, 4.9 Hz, 3H).

# **General Procedure for Ether Synthesis (FAE 1 to 5)**

A 500 mL round bottom flask was charged with **FA alcohol** (1 equiv.), KI (0.1 equiv.) and THF, then cooled to 0 °C with an ice bath. To this mixture, 60% NaH dispersion in mineral oil (1.2-1.5 equiv.) was added portion-wise over 20 min and stirred for 10 min. The requisite alkyl halide (1.3-2.0 equiv.) was added via a syringe and the reaction mixture was brought to reflux for 16 h. Once the starting material was consumed as determined by TLC and GCMS, the reaction was cooled to 0 °C and quenched via slow addition of H<sub>2</sub>O (50 mL), extracted with hexanes (2 x 50 mL), washed with saturated NaCl solution (50 mL), dried using anhydrous MgSO<sub>4</sub>, filtered, and concentrated *in vacuo*. The crude reaction mixture was purified via distillation. All reported reaction yields are unoptimized.

Compound **FAE-1**: Bulb-to-bulb distillation under reduced pressure (390 mTorr, 107–120°C) to afford **FAE-1** (80.1 g, 83%) as a colorless oil.  $^{1}$ H NMR (500 MHz, CDCl<sub>3</sub>)  $\delta$  5.38-5.26 (m, 2.6H), 3.33 (t, J = 6.7 Hz, 2H), 3.29 (s, 3H), 2.74 (t, J = 6.8 Hz, 1H), 2.05-1.96 (m, 3H), 1.57-1.50 (m, 2H), 1.35-1.20 (m, 19H), 0.86 (q, J = 6.4 Hz, 3H).

Compound **FAE-2**: Bulb-to-bulb distillation under reduced pressure (400 mTorr, 114–126°C) to afford **FAE-2** (56.0 g, 84%) as a colorless oil.  $^{1}$ H NMR (500 MHz, CDCl<sub>3</sub>)  $\delta$  5.38-5.26 (m, 2.6H), 3.46 (q, J = 7.0 Hz, 2H), 3.39 (t, J = 6.8 Hz, 2H), 2.77 (t, J = 6.4 Hz, 1H), 2.07-1.98 (m, 3H), 1.59-1.53 (m, 2H), 1.37-1.23 (m, 19H), 1.19 (t, J = 7.0 Hz, 3H), 1.90-0.86 (m, 3H).

Compound **FAE-3**: Bulb-to-bulb distillation under reduced pressure (400 mTorr, 114–126°C) to afford **FAE-3** (56.0 g, 84%) as a colorless oil. <sup>1</sup>H NMR (500 MHz, CDCl<sub>3</sub>)  $\delta$  5.38-5.26 (m, 2.6H), 3.39 (q, J = 6.7 Hz, 4H), 2.77 (t, J = 6.8 Hz, 1H), 2.07-1.98 (m, 3H), 1.58-1.51 (m, 4H), 1.39-1.25 (m, 21H), 0.92 (t, J = 7.4 Hz, 3H), 0.89-0.86 (m, 3H).

Compound **FAE-4**: Bulb-to-bulb distillation under reduced pressure (1.20 Torr, 136–153°C) to afford **FAE-4** (33.2 g, 45%) as a pale- yellow oil. <sup>1</sup>H NMR (500 MHz, CDCl<sub>3</sub>)  $\delta$  5.40-5.28 (m, 2.6H), 3.39 (t, J = 6.5 Hz, 2H), 3.16 (d, J = 6.7 Hz, 2H), 2.77 (t, J = 6.5 Hz, 1H), 2.07-1.98 (m, 3H), 1.85 (septet, J = 6.7 Hz, 1H), 1.57-1.50 (m, 2H), 1.35-1.20 (m, 19H), 0.90 (d, J = 6.8 Hz, 6H), 0.86 (q, J = 6.0 Hz, 3H).

Compound FAE-5: Bulb-to-bulb distillation under reduced pressure (390 mTorr, 129–149°C) to afford FAE-5 (40.0 g, 66%) as a colorless oil. <sup>1</sup>H NMR (500 MHz, CDCl<sub>3</sub>)  $\delta$  5.40-5.28 (m, 2.6H), 3.42 (t, J = 6.5 Hz, 2H), 3.38 (t, J = 6.7 Hz, 2H), 2.77 (t, J = 6.5 Hz, 1H), 2.07-1.98 (m, 3H), 1.69 (septet, J = 6.7 Hz, 1H), 1.57-1.50 (m, 2H), 1.46 (q, J = 6.8 Hz, 2H), 1.35-1.20 (m, 19H), 0.90 (d, J = 6.6 Hz, 6H), 0.86 (q, J = 6.0 Hz, 3H).

# **Fuel Property Testing**

Fuel properties of the various molecules investigated in this study were tested following ASTM protocols in partnership with Intertek Inc in Benecia, CA, which is a commercial testing facility. Derived Cetane Number (DCN) was determined by Ignition Quality Test (IQT) according to ASTM D6890 protocol (ASTM-D6890-16e1, 2016)<sup>20</sup>. Cloud Point (CP) was determined according to ASTM D2500 protocol (ASTM-D2500-17a, 2017)<sup>21</sup>. Pour Point (PP) according to ASTM D97 protocol (ASTM-D97-17b, 2017)<sup>22</sup>. Cold Filter Plug Point (CFPP) according to ASTM D6371 (ASTM-D6371-17a, 2017)<sup>23</sup>. Higher Heating Value (HHV) was determined by ASTM 4809 (ASTM-4809-18, 2018)<sup>24</sup>, except for FAE-1, which was determined by D240 protocol (ASTM-D240-19, 2019)<sup>25</sup>. The Lower Heating Value (LHV) was calculated based on the

HHV using the equation developed by Lloyd (referenced in ASTM D240 method) which is shown below as **Equation 1**.<sup>26</sup>

$$LHV [M]/kg] = HHV [M]/kg] - (0.2122 \times hydrogen [mass \%])$$
 (1)

# Measurement of Yield Sooting Index (YSI)

The sooting tendencies of the FAEs and other related compounds were measured using the previously developed yield-based approach.<sup>27</sup> The specific procedures and apparatus used in this study were identical to those in McEnally et al 2019.<sup>28</sup> It consisted of three steps: (1) 1000 ppm of n-heptane, toluene, and each test compound were sequentially doped into the fuel of a nitrogen-diluted methane/air coflow nonpremixed flame; (2) the maximum soot concentration was measured in each flame with line-of-sight spectral radiance (LSSR); and (3) these concentrations were rescaled into a yield sooting index (YSI) defined by **Equation 2**:

$$YSI_{TC} = (YSI_{TOL} - YSI_{HEP}) \times \frac{LSSR_{TC} - LSSR_{HEP}}{LSSR_{TOL} - LSSR_{HEP}} + YSI_{HEP}$$
 (2)

The subscripts TC, TOL, and HEP refer to the test compound, toluene, and n-heptane respectively. This rescaling method removes sources of systematic uncertainty such as errors in the gas-phase reactant flow rates. Furthermore, it allows the new results to be quantitatively compared with a database that contains measured YSIs for hundreds of organic compounds. The parameters YSI<sub>TOL</sub> and YSI<sub>HEP</sub> are constants that define the YSI scale; their values—170.9 and 36.0—were taken from the database<sup>29</sup> so that the newly measured YSIs would be on the same scale. The systematic uncertainty in YSI is  $\pm 2\%$ , which is dominated by the uncertainty in the mass densities of the samples. These were predicted using the group contribution method of Mathieu and Bouteloup 2016.<sup>30</sup> Isooctane was used as an internal standard and measured 10 times during this study. Its

measured values were consistent over time with a variation of  $\pm 2.8\%$  (2 standard deviations). Thus the total uncertainty in the measured YSIs is  $\pm 5\%$ ; the average value for isooctane (64.3) agrees to within this uncertainty with earlier measurements (61.7).<sup>31</sup> YSI characterizes the sooting tendency per mole; to determine the sooting tendency per mass (YSI/kg) and per heat release (YSI/MJ) – which are more relevant to diesel engines – the measured YSIs were divided by the molecular weight and LHV respectively. The molar mass of the C18:02 fatty acid (linoleic acid) was used since it was the dominant fatty acid in the mixture as shown in **Table 1**. Uncertainty for the YSI/MJ metric accounts for error in both inputs (YSI and LHV).

### **RESULTS AND DISCUSSION**

While extensive research has been done exploring fatty acid derived esters as fuels for compression ignition engines, <sup>32, 33</sup> investigations into molecules containing fatty carbon chains with non-ester functionality have been limited. <sup>32-34</sup> To understand the fuel property implications of non-traditional fatty acid derived fuels as compared to traditional biodiesel (represented by **FA ethyl ester**), this work first investigated three fatty alkyl congeners: acetate, alcohol, and ether (**Figure 1**). For each compound a two-carbon group was used for carbon number parity across the molecular classes, with the exception of **FA alcohol** (which by definition only has an H atom on the side opposite the fatty carbon chain.

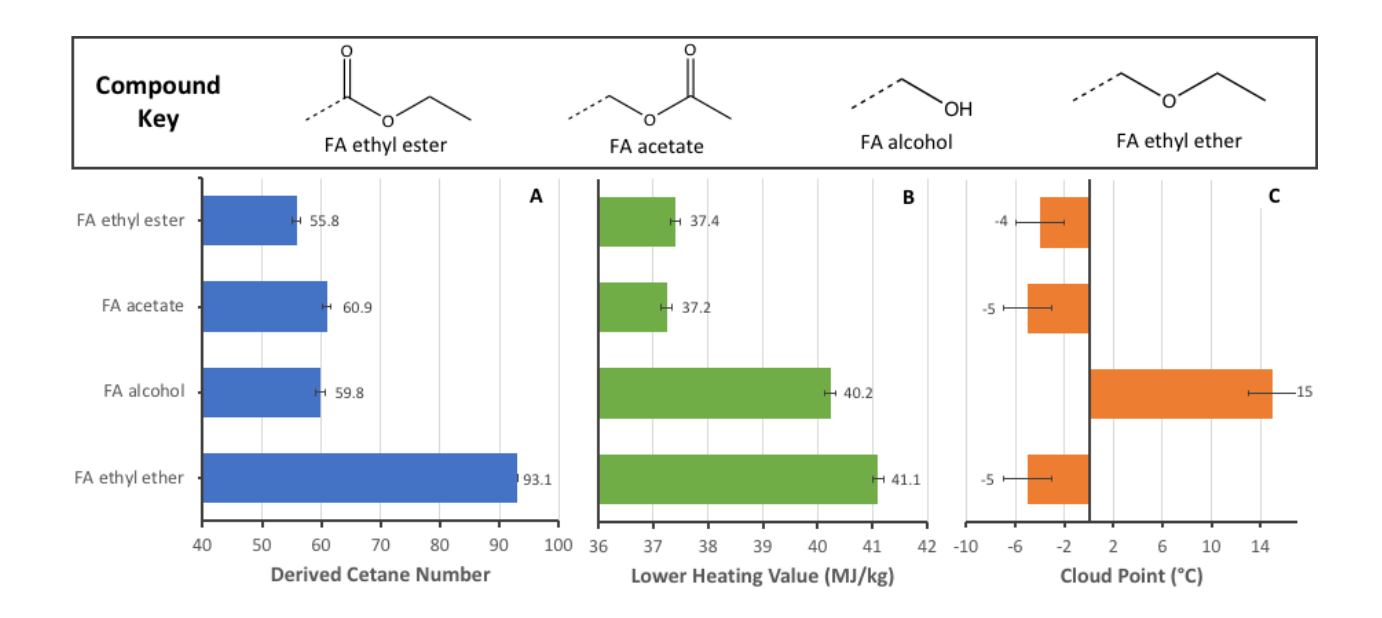


**Figure 1.** The effect of oxidation state on fuel properties: (A) Derived Cetane Number, (B) Lower Heating Value, (C) and Cloud Point (CP). Error bars are the reproducibility metrics as outlined in the respective ASTM method.<sup>20</sup>

**FA alcohol** has reasonable DCN and LHV, but a prohibitively high CP, eliminating it from consideration. The **FA ethyl ester** and **FA acetate** have similar properties, with the **FA acetate** demonstrating higher DCN. Within the series, **FA ethyl ether** has the strongest DCN performance. While DCN values >75 are outside the calibration range of the method and therefore cannot be quantitatively compared, the DCN value of 93.1 represents a significant qualitative improvement over the other compounds investigated. The ethyl ether also has the highest LHV and a lower CP, suggesting that ether functional groups are promising candidates as fatty acid based fuels.

Soot formation is another critical fuel property to consider when evaluating biofuel candidates for compression ignition engines. One well documented benefit of oxygenated fuels is their ability to reduce soot formation when blended into traditional diesel base fuels due to their lack of aromatic

constituents and the atomic oxygen being able to sequester carbon atoms as CO/CO<sub>2</sub>. <sup>35-37</sup> This can lead to cost reductions for the after-treatment systems used on heavy duty engines. <sup>38</sup>

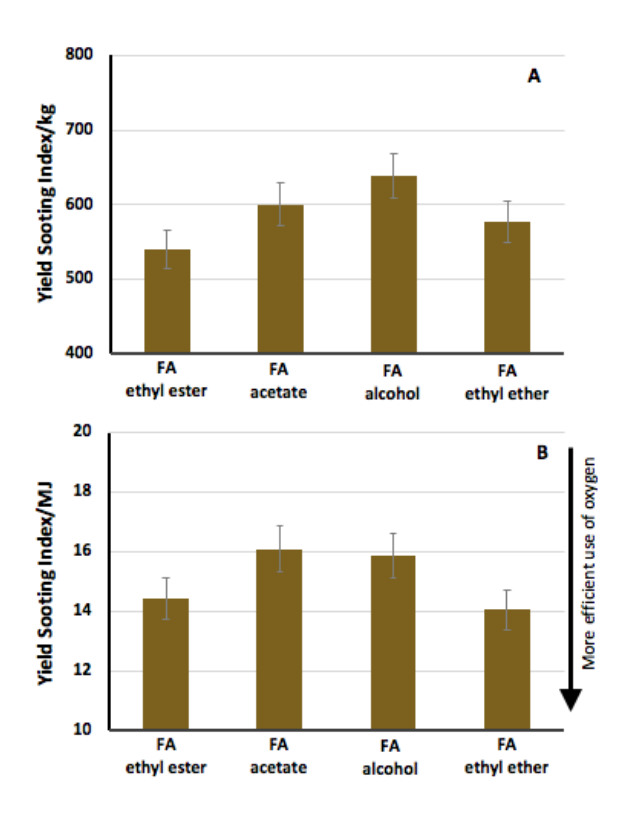


**Figure 2.** Evaluation of Yield Sooting Index (YSI) of various potential oxidation states of fatty alkyl based biofuels ratioed to (A) molecular mass and (B) lower heating value. **FA ethyl ester** and **FA ethyl ether** demonstrate the strongest YSI performance on both a per kg and per MJ basis. Error bars represent the  $\pm 5\%$  uncertainty described in the methods.

While sooting tendencies generally correlate inversely to the mass percent of oxygen,<sup>39</sup> the sooting performance of oxygenated biofuels is more nuanced than just C:O ratio or oxygen mass %, a phenomenon previously suggested.<sup>40</sup> **FA ethyl ester** and **FA acetate** have the same molecular formula and oxygen mass fraction of 10.3%, yet **FA acetate** forms significantly more soot/kg than **FA ethyl ester** (**Figure 2A**). Additionally, **FA ethyl ether** has a lower oxygen mass percent than

both **FA acetate** and **FA alcohol**, yet forms less soot per kg. A likely explanation is that for **FA ether** the oxygen interrupts the carbon chain generating smaller alkyl fragments during pyrolysis, whereas for **FA alcohol** the oxygen atom is terminal to the alkyl chain, and **FA acetate** allows sixmembered eliminations reactions that produce large unsaturated hydrocarbons (**Figure 3**). Al. 42 These results show that the specific oxygen functionality has an important impact on soot formation as previously suggested by Mueller et al. Since increasing oxygen content and thereby decreasing C:O ratio has a well-established negative impact on a fuel's LHV, finding the most efficient form of oxygen provides value through net fuel properties optimization. When considered as a ratio of soot formation to energy density, **FA ethyl ether** and **FA ethyl ester** are the strongest performers and demonstrate the most efficient use of oxygen when considering the soot formation/energy density tradeoff.

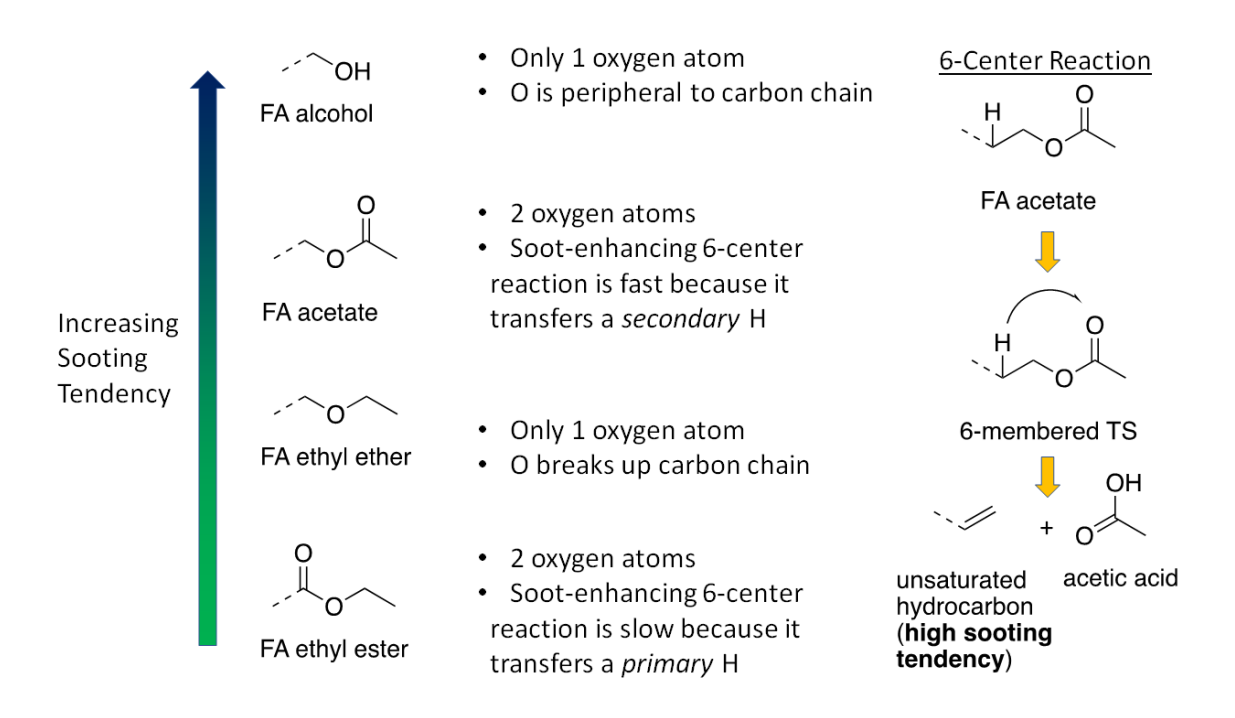


Figure 3. Potential soot formation pathways for the different oxidation states investigated.

Based on the strong performance of **FA ethyl ether** described above, the broader class of molecules herein described as Fatty Alkyl Ethers (FAEs) was investigated further by determining the impact that varying the shorter alkyl chain has on the fuel properties of interest (**Figure 4**). C1-C5 straight and branched carbon chains were selected because these structures can be derived sustainably from biomass at industrial scales in the form of alcohols.<sup>43-45</sup>

Figure 4. Synthesis of biodiesel derived ethers composed of a mixture of lipids.

Given that the lipid content of vegetable oils and fats are composed of a mixture of alkyl chain lengths and unsaturated double bonds, the derived biodiesel is also a mixture of esters (**Figure 4**). This makes it difficult to define the fuel properties of biodiesel precisely. The elements of unsaturation in the lipid profile have been shown to correlate with the cetane number and cloud point (CP) of biodiesel. This adds a complication when evaluating new lipid derived fuels in comparison to biodiesel. For this reason, the new fuels described in this paper are derived from the same batch of B100 biodiesel, as described in the methods section, to achieve a fixed lipid composition. In this way, a comparison of the fuel properties is limited to the difference in the terminal functional group, and not the lipid profile.

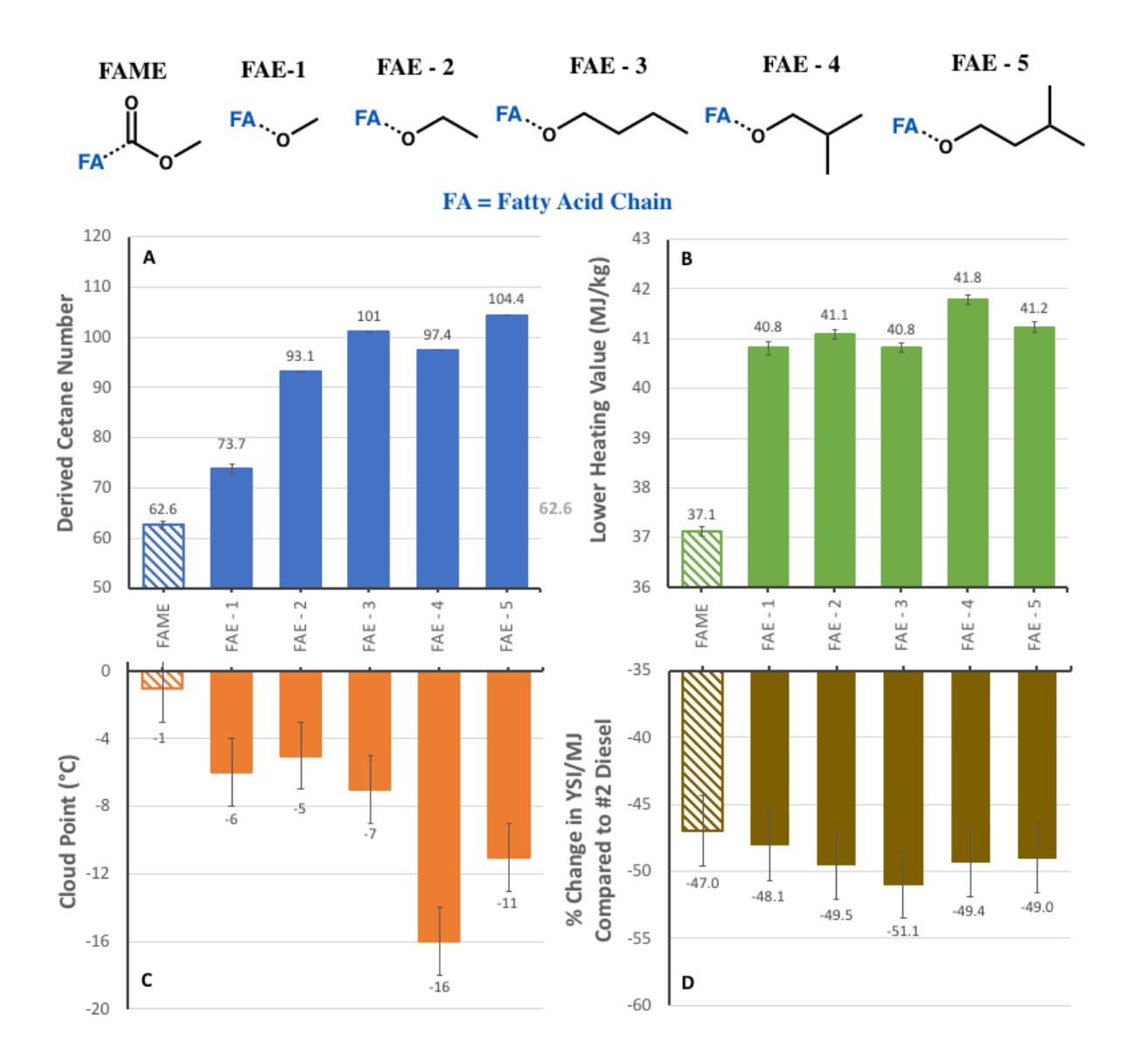


Figure 5. Fatty Alkyl Ether (FAE) derivatives evaluated for fuel properties: (A) Derived Cetane Number (DCN), (B) Lower Heating Value (LHV), (C) Cloud Point (CP), and (D) reduction in YSI/MJ compared to diesel fuel. All FAEs show a significant improvement as compared to a FAME control in every property except YSI/MJ, where a nominal improvement was measured but is within the higher uncertainty of that measurement. Increasing carbon chain length improved DCN, LHV, and CP, while increased branching lowered DCN, but improved LHV and CP. Error

bars in A-C represent established repeatability of the results as defined by the corresponding ASTM method. Error for (D) is discussed in the methods section.

As a general trend, increasing the length of the alkyl chain improves all the properties investigated, while increased branching increases energy density and lowers cloud point (CP) but decreases cetane number and increases YSI (Figure 5). While FAE 2-5 had DCN values outside the calibration range for the method, the variation in ignition delay (ID) times suggests there is a significant difference between their autoignition tendencies (Table S1). An interesting phenomenon was observed within the series FAE 1-3. In this series, increasing the length of the short straight chained alkyl group decreases the YSI per kg of fuel by a small margin.

When evaluating the branched compounds **FAE 4** and **5**, a gain in DCN, LHV and cloud point is achieved over the linear congeners. The improvement is most evident when comparing the four carbon isomers **FAE 3** and **FAE 4**, which show that a single element of branching on the alkyl group can provide a  $\Delta T_{cp}$  of -9 °C. It is notable that all of the FAE compounds offer an improvement over **FAME** in DCN but the greatest benefit is seen in **FAE 5** with a DCN = 104.4, a significant improvement over the **FAME** control fuel.

While cloud point is a well-established metric for evaluating the cold flow-properties of diesel fuels, pour point (PP) and cold filter plug point (CFPP) are two other properties that are also important to consider. Comparison of the three different cold flow properties between methyl ether **FAE 1** and isoamyl ether **FAE 5** highlight some differences between the types of cold flow (**Figure 6**). While in each case the measured value of **FAE 5** was lower than that of **FAE 1**, the level of improvement varied across the different tests. The improvement in PP was not outside the repeatability of measurement, while both CP and CFPP saw significant improvements. Of all the

cold flow properties, the CFPP was improved the most from **FAE 1** to **FAE 5**, with a decrease of 6 °C observed. This is an important result because some analyses suggest that CFPP may be the most critical property for engine performance.<sup>47</sup> This indicates that FAEs may have even better cold flow improvements compared to biodiesel than is suggested from the cloud point data in **Figure 5**.

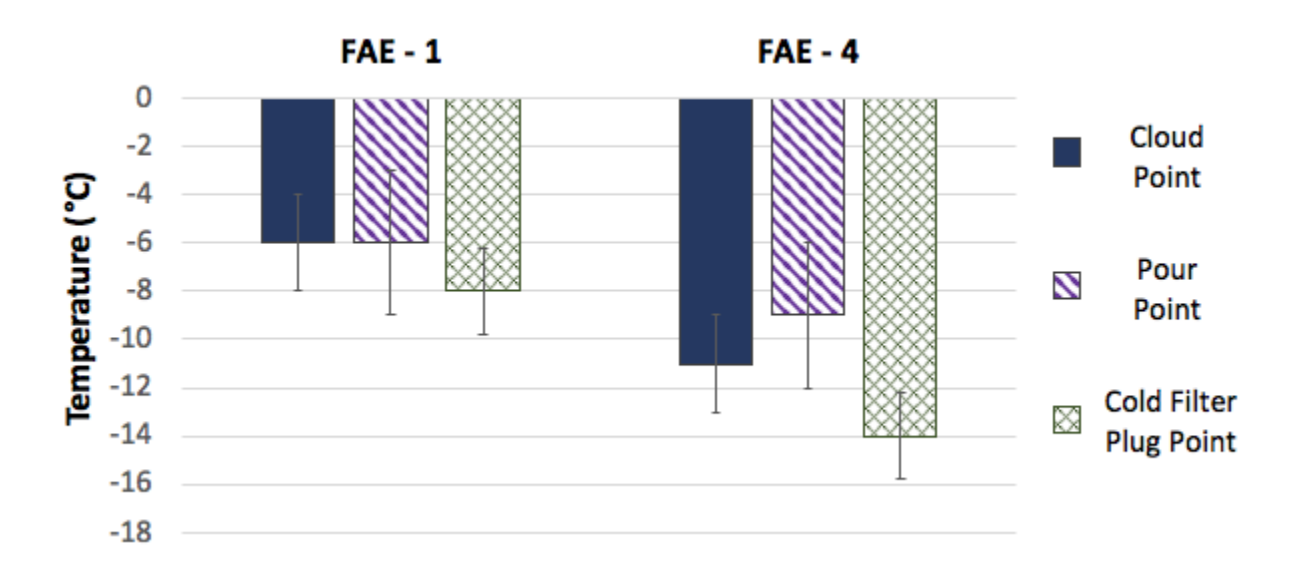


**Figure 6.** Complete cold flow comparison between methyl ether and isoamyl ether. B100 methyl ether has a non-significant improvement in PP, but significantly improved CP and CFPP. Error bars represent the stated repeatability of the measurements outlined in the ASTM methods.

### **CONCLUSIONS**

In this study, a survey of molecules derived from lipids with various terminal functional groups was conducted that established a beneficial improvement on combustion fuel properties with alkyl ether congeners over acetate, alcohol and ester. After an initial survey of various terminal functional groups derived from fatty acids as compression ignition engines fuels, it was evident that alkyl ethers possessed benefits over esters and alcohols in all fuel property categories. Within

the initial series of varying terminal groups, an interesting sooting phenomenon was observed where an ether, which contains less oxygen than an acetate congener, emits less soot on a per mass basis - a reversal in a common trend due to the intramolecular nature of the mechanism on soot formation. A further investigation into fatty alkyl ethers regarding the effect of chain length and branching of the alkyl group was carried out which revealed that increasing the carbon chain generally improved all properties investigated, while branching led to significant improvements in cold flow, minor improvements in energy density, and slightly worse performance in cetane number and sooting tendency. All fatty alkyl ethers investigated showed improvements in DCN, LHV, sooting and cold flow as compared to a FAME (B100) control fuel. These results demonstrate the potential for fatty alkyl ethers for use as all-weather fuels, while also reducing soot emissions and increasing engine performance and fuel economy as compared to traditional biodiesel. Future work should focus on synthesis of FAEs directly from triglycerides or fatty acids, utilizing chemistries compatible with large scale industrial operations to match the scale of fuel production.

## **Funding Sources**

This research was conducted as part of the Co-Optimization of Fuels & Engines (Co-Optima) project sponsored by the U.S. Department of Energy (DOE) Office of Energy Efficiency and Renewable Energy (EERE), Bioenergy Technologies and Vehicle Technologies Offices. Sandia National Laboratories is a multi-mission laboratory managed and operated by National Technology and Engineering Solutions of Sandia, LLC., a wholly owned subsidiary of Honeywell International, Inc., for the U.S. Department of Energy's National Nuclear Security Administration under contract DE-NA0003525.

## Acknowledgment

The authors would like to acknowledge Lisa Fouts and Robert McCormick at the National Renewable Energy Laboratory (NREL) in Golden, CO for generously donating the Fatty Acid Methyl Ester used as a fuel property control and as a starting material for the synthesis of FAE's.

### References

- 1. H.R. 6: Energy Independence and Security Act of 2007. In *P.L. 110-140*, Congress, t. U. S., Ed. 2007.
- 2. Standard Specification for Biodiesel Fuel Blend Stock (B100) for Middle Distillate Fuels. In *ASTM D6751-19*, 2019.
- 3. Renewable Fuel Standard Program: Standards for 2014, 2015, and 2016 and Biomass-Based Diesel Volume for 2017. In 40 CFR 80, Agency, E. P., Ed. 2015.
- 4. Shrestha, D.; Van Gerpen, J.; Thompson, J.; Zawadzki, A. In *Cold flow properties of biodiesel* and effect of commercial additives, 2005 ASAE Annual Meeting, 2005; American Society of Agricultural and Biological Engineers: 2005; p 1.
- 5. Monirul, I.; Masjuki, H.; Kalam, M.; Zulkifli, N.; Rashedul, H.; Rashed, M.; Imdadul, H.; Mosarof, M., A comprehensive review on biodiesel cold flow properties and oxidation stability along with their improvement processes. *RSC advances* **2015**, 5, (105), 86631-86655.
- 6. Bolonio, D.; Llamas, A.; Rodríguez-Fernández, J.; Al-Lal, A. M.; Canoira, L.; Lapuerta, M.; Gómez, L., Estimation of cold flow performance and oxidation stability of fatty acid ethyl esters from lipids obtained from Escherichia coli. *Energy & Fuels* **2015**, 29, (4), 2493-2502.
- 7. Monroe, E.; Shinde, S.; Carlson, J. S.; Eckles, T. P.; Liu, F.; Varman, A. M.; George, A.; Davis, R. W., Superior performance biodiesel from biomass-derived fusel alcohols and low grade oils: Fatty acid fusel esters (FAFE). *Fuel* **2020**, 268.
- 8. Huo, X.; Huq, N. A.; Stunkel, J.; Cleveland, N. S.; Starace, A. K.; Settle, A. E.; York, A. M.; Nelson, R. S.; Brandner, D. G.; Fouts, L., Tailoring diesel bioblendstock from integrated catalytic upgrading of carboxylic acids: A "fuel property first" approach. *Green Chemistry* **2019**, 21, (21), 5813-5827.
- 9. Dahmen, M.; Marquardt, W., Model-based design of tailor-made biofuels. *Energy & Fuels* **2016**, 30, (2), 1109-1134.
- 10. Dunn, J. B.; Biddy, M.; Jones, S.; Cai, H.; Benavides, P. T.; Markham, J.; Tao, L.; Tan, E.; Kinchin, C.; Davis, R., Environmental, economic, and scalability considerations and trends of selected fuel economy-enhancing biomass-derived blendstocks. *ACS Sustainable Chemistry & Engineering* **2018**, 6, (1), 561-569.
- 11. Staples, O.; Leal, J. H.; Cherry, P. A.; McEnally, C. S.; Pfefferle, L. D.; Semelsberger, T. A.; Sutton, A. D.; Moore, C. M., Camphorane as a renewable diesel blendstock produced by cyclodimerization of myrcene. *Energy & Fuels* **2019**, 33, (10), 9949-9955.
- 12. Lee, W. S.; Chua, A. S. M.; Yeoh, H. K.; Ngoh, G. C., A review of the production and applications of waste-derived volatile fatty acids. *Chemical Engineering Journal* **2014**, 235, 83-99.
- 13. Huq, N. A.; Huo, X.; Hafenstine, G. R.; Tifft, S. M.; Stunkel, J.; Christensen, E. D.; Fioroni, G. M.; Fouts, L.; McCormick, R. L.; Cherry, P. A.; McEnally, C. S.; Pfefferle, L. D.;

- Wiatrowski, M. R.; Benavides, P. T.; Biddy, M. J.; Connatser, R. M.; Kass, M. D.; Alleman, T. L.; St John, P. C.; Kim, S.; Vardon, D. R., Performance-advantaged ether diesel bioblendstock production by a priori design. *Proc Natl Acad Sci U S A* **2019**.
- 14. Bailey, B.; Eberhardt, J.; Goguen, S.; Erwin, J., Diethyl ether (DEE) as a renewable diesel fuel. *SAE transactions* **1997**, 1578-1584.
- 15. Damyanov, A.; Hofmann, P.; Geringer, B.; Schwaiger, N.; Pichler, T.; Siebenhofer, M., Biogenous ethers: Production and operation in a diesel engine. *Automotive and Engine Technology* **2018**, 3, (1-2), 69-82.
- 16. Rorrer, J. E.; Bell, A. T.; Toste, F. D., Synthesis of Biomass-Derived Ethers for Use as Fuels and Lubricants. *ChemSusChem* **2019**, 12, (13), 2835-2858.
- 17. Xiang, J.; Shang, M.; Kawamata, Y.; Lundberg, H.; Reisberg, S. H.; Chen, M.; Mykhailiuk, P.; Beutner, G.; Collins, M. R.; Davies, A.; Del Bel, M.; Gallego, G. M.; Spangler, J. E.; Starr, J.; Yang, S.; Blackmond, D. G.; Baran, P. S., Hindered dialkyl ether synthesis with electrogenerated carbocations. *Nature* **2019**, 573, (7774), 398-402.
- 18. Beddoe, R. H.; Andrews, K. G.; Magne, V.; Cuthbertson, J. D.; Saska, J.; Shannon-Little, A. L.; Shanahan, S. E.; Sneddon, H. F.; Denton, R. M., Redox-neutral organocatalytic Mitsunobu reactions. *Science* **2019**, 365, (6456), 910-914.
- 19. Fioroni, G.; Fouts, L.; Luecke, J.; Vardon, D.; Huq, N.; Christensen, E.; Huo, X.; Alleman, T.; McCormick, R.; Kass, M., Screening of potential biomass-derived streams as fuel blendstocks for mixing controlled compression ignition combustion. *SAE International Journal of Advances and Current Practices in Mobility* **2019**, 1, (2019-01-0570), 1117-1138.
- 20. ASTM-D6890-16e1, Standard Test Method for Determination of Ignition Delay and Derived Cetane Number (DCN) of Diesel Fuel Oils by Combustion in a Constant Volume Chamber. In ASTM International, West Conshohocken, PA: 2016.
- 21. D2500-17a, A., Standard Test Method for Cloud Point of Petroleum Products and Liquid Fuels. *ASTM International* **2017**, West Conshohocken, PA.
- 22. D97-17b, A., Standard Test Method for Pour Point of Petroleum Products. *ASTM International* **2017**, West Conshohocken, PA.
- 23. D6371-17a, A., Standard Test Method for Cold Filter Plugging Point of Diesel and Heating Fuels. *ASTM International* **2017**, West Conshohocken, PA.
- 24. D4809-18, A., Standard Test Method for Heat of Combustion of Liquid Hydrocarbon Fuels by Bomb Calorimeter (Precision Method). *ASTM International* **2018**, West Conshohocken, PA.
- 25. ASTM-D240-19, Standard Test Method for Heat of Combustion of Liquid Hydrocarbon Fuels by Bomb Calorimeter. In ASTM International, West Conshohocken, PA: 2019.
- 26. Lloyd, W. G.; Davenport, D. A., Applying thermodynamics to fossil fuels: Heats of combustion from elemental compositions. *Journal of Chemical Education* **1980**, 57, (1), 56.
- 27. McEnally, C. S.; Pfefferle, L. D., Improved sooting tendency measurements for aromatic hydrocarbons and their implications for naphthalene formation pathways. *Combustion and Flame* **2007**, 148, (4), 210-222.
- 28. McEnally, C. S.; Xuan, Y.; John, P. C. S.; Das, D. D.; Jain, A.; Kim, S.; Kwan, T. A.; Tan, L. K.; Zhu, J.; Pfefferle, L. D., Sooting tendencies of co-optima test gasolines and their surrogates. *Proceedings of the Combustion Institute* **2019**, 37, (1), 961-968.
- 29. McEnally, C.; Das, D.; Pfefferle, L., Yield Sooting Index Database Vol. 2: Sooting Tendencies of a Wide Range of Fuel Compounds on a Unified Scale. In Harvard Dataverse: 2017.

- 30. Mathieu, D.; Bouteloup, R. m., Reliable and versatile model for the density of liquids based on additive volume increments. *Industrial & Engineering Chemistry Research* **2016**, 55, (50), 12970-12980.
- 31. Das, D. D.; St. John, P. C.; McEnally, C. S.; Kim, S.; Pfefferle, L. D., Measuring and predicting sooting tendencies of oxygenates, alkanes, alkenes, cycloalkanes, and aromatics on a unified scale. *Combustion and Flame* **2018**, 190, 349-364.
- 32. Demirbas, A., Importance of biodiesel as transportation fuel. *Energy policy* **2007**, 35, (9), 4661-4670.
- 33. Pinzi, S.; Garcia, I.; Lopez-Gimenez, F.; Luque de Castro, M.; Dorado, G.; Dorado, M., The ideal vegetable oil-based biodiesel composition: a review of social, economical and technical implications. *Energy & Fuels* **2009**, 23, (5), 2325-2341.
- 34. Runguphan, W.; Keasling, J. D., Metabolic engineering of Saccharomyces cerevisiae for production of fatty acid-derived biofuels and chemicals. *Metabolic Engineering* **2014**, 21, 103-113.
- 35. Mueller, C. J.; Pitz, W. J.; Pickett, L. M.; Martin, G. C.; Siebers, D. L.; Westbrook, C. K., Effects of Oxygenates on Soot Processes in DI Diesel Engines: Experiments and Numerical Simulations. *SAE Transactions* **2003**, 112, 964-982.
- 36. Nilsen, C. W.; Biles, D. E.; Mueller, C. J., Using Ducted Fuel Injection to Attenuate Soot Formation in a Mixing-Controlled Compression Ignition Engine. *SAE International Journal of Engines (Online)* **2019**, 12, (SAND-2019-1518J; SAND-2018-12942J).
- 37. Pepiot-Desjardins, P.; Pitsch, H.; Malhotra, R.; Kirby, S.; Boehman, A. L., Structural group analysis for soot reduction tendency of oxygenated fuels. *Combustion and Flame* **2008**, 154, (1-2), 191-205.
- 38. Ou, L.; Cai, H.; Seong, H. J.; Longman, D. E.; Dunn, J. B.; Storey, J. M.; Toops, T. J.; Pihl, J. A.; Biddy, M.; Thornton, M., Co-optimization of Heavy-Duty Fuels and Engines: Cost Benefit Analysis and Implications. *Environmental science & technology* **2019**, 53, (21), 12904-12913.
- 39. Musculus, M. P.; Dec, J. E.; Tree, D. R., Effects of Fuel Parameters and Diffusion Flame Lift-Off on Soot Formation in a Heavy-Duty DI Diesel Engine. In SAE International: 2002.
- 40. Curran, H. J.; Fisher, E. M.; Glaude, P. A.; Marinov, N. M.; Pitz, W. J.; Westbrook, C. K.; Layton, D. W.; Flynn, P. F.; Durrett, R. P.; zur Loye, A. O.; Akinyemi, O. C.; Dryer, F. L., Detailed Chemical Kinetic Modeling of Diesel Combustion with Oxygenated Fuels. In SAE International: 2001.
- 41. McEnally, C. S.; Pfefferle, L. D., Sooting tendencies of oxygenated hydrocarbons in laboratory-scale flames. *Environmental science & technology* **2011**, 45, (6), 2498-2503.
- 42. McEnally, C. S.; Pfefferle, L. D., Fuel decomposition and hydrocarbon growth processes for oxygenated hydrocarbons: butyl alcohols. *Proceedings of the Combustion Institute* **2005**, 30, (1), 1363-1370.
- 43. Liu, F.; Lane, P.; Hewson, J. C.; Stavila, V.; Tran-Gyamfi, M. B.; Hamel, M.; Lane, T. W.; Davis, R. W., Development of a closed-loop process for fusel alcohol production and nutrient recycling from microalgae biomass. *Bioresource Technology* **2019**, 283, 350-357.
- 44. Liu, F.; Wu, W.; Tran-Gyamfi, M. B.; Jaryenneh, J. D.; Zhuang, X.; Davis, R. W., Bioconversion of distillers' grains hydrolysates to advanced biofuels by an Escherichia coli co-culture. *Microbial Cell Factories* **2017**, 16, (1), 192.

- 45. DeRose, K.; Liu, F.; Davis, R. W.; Simmons, B. A.; Quinn, J. C., Conversion of Distiller's Grains to Renewable Fuels and High Value Protein: Integrated Techno-Economic and Life Cycle Assessment. *Environmental science & technology* **2019**, 53, (17), 10525-10533.
- 46. Hoekman, S. K.; Broch, A.; Robbins, C.; Ceniceros, E.; Natarajan, M., Review of biodiesel composition, properties, and specifications. *Renewable and Sustainable Energy Reviews* **2012**, 16, (1), 143-169.
- 47. Chiu, C.-W.; Schumacher, L. G.; Suppes, G. J., Impact of cold flow improvers on soybean biodiesel blend. *Biomass and Bioenergy* **2004**, 27, (5), 485-491.